

Short and long term evolution of a stellar disk around a massive black hole: The role of binaries, the cusp and stellar evolution

Diego N. Mikhaloff & Hagai B. Perets

Physics department, Technion - Israel institute of Technology, Haifa, Israel 3200002
dmikhaloff@tx.technion.ac.il; hperets@physics.technion.ac.il

11 September 2021

ABSTRACT

We study the dynamical evolution of a stellar disk orbiting a massive black hole. We explore the role of two-body relaxation, mass segregation, stellar evolution and binary heating in affecting the disk evolution, and consider the impact of the nuclear cluster structure and the stellar-disk mass-function. We use analytic arguments and numerical calculations, and apply them to study the evolution of a stellar disk (similar to that observed in the Galactic center; GC), both on the short (few Myr) and longer (100 Myr) evolutionary timescales. We find the dominant processes affecting the disk evolution are two-body relaxation and mass segregation where as binary heating have only a little contribution. Massive stars play a dominant role in kinematically heating low mass stars, and driving them to high eccentricities/inclinations. Multi-mass models with realistic mass-functions for the disk stars show the disk structure to be mass stratified, with the most massive stars residing in thinner structures. Stellar evolution plays an important role in decreasing the number of massive stars with time, thereby leading to slower relaxation, where the remnant compact objects of these stars are excited to higher eccentricities/inclinations. At these later evolutionary stages dynamical heating by the nuclear cluster plays a progressively more important role. We conclude that the high eccentricities and high inclination observed for the majority on the young O-stars in the Galactic Center suggest that the disk stars had been formed with initially high eccentricities, or that collective or secular processes (not explored here) dominate the disk evolution. The latter processes are less likely to produce mass stratification in the disk; detailed study of the mass-dependent kinematic properties of the disk stars could therefore provide a handle on the processes that dominate its evolution. Finally, we find that the disk structure is expected to keep its coherency, and be observed as a relatively thin disk even after 100 Myrs; two-body relaxation is too inefficient for the disk to assimilate into the nuclear cluster on such timescales. It therefore suggests earlier disks now containing only older, lower mass stars might still be observed in the Galactic center, unless destroyed/smeared by other non-two-body relaxation processes.

Key words: Galaxy: centre – galaxies: nuclei – Galaxy: structure – stars: kinematics and dynamics – Galaxy: nucleus

1 INTRODUCTION

Stellar disks are known to exist around massive black holes (MBHs) in galactic nuclei, and are typically composed of relatively young stellar populations. Observations of the central parsec of the Milky-Way Galaxy show more than 100 young WR, O and B stars (Paumard et al. 2006), likely formed $\sim 4 - 7$ Myr ago. These stars are found between $\sim 0.04 - 0.5$ pc from the MBH, with $\sim 20\%$ of which reside in a disk-like structure, and are observed to have mean high eccentricity of $\langle e \rangle \sim 0.3 - 0.4$. Stellar disks might therefore be a frequent phenomena in galactic nuclei. Such disks are thought to form following the infall of gaseous material, and its formation of a gaseous disk. Such a disk can later fragment to form a stellar disk (Hobbs & Nayakshin 2009, and references therein). Here we

explore the dynamical evolution of such stellar disks, and focus on disks similar to that observed in the Galactic center.

Alexander et al. (2007) have been the first to describe the behavior of a stellar disk around a MBH. They used an analytic approach, and then verified and calibrated them through the use of N-body simulations. The analytic model they devised includes the effects of two-body relaxation, and included simple multi-mass models (two or three populations). Their N-body simulations also included a simplified stellar evolution.

Later studies by Cuadra et al. (2008), Perets et al. (2008) and Lückmann et al. (2009) performed additional N-body simulations and considered additional components and/or more realistic aspects. Cuadra et al. (2008) included stellar binaries in the disk, the role of a putative intermediate mass black holes, and initially ec-

arXiv:1504.05951v1 [astro-ph.GA] 22 Apr 2015

centric disks. Kocsis & Tremaine (2011) discussed the evolution of the stellar disk, mainly focusing on the effects of resonant relaxation (Rauch & Tremaine 1996), not considered here. The influence of the stellar cusp was studied numerically by Perets et al. (2008) and Löckmann et al. (2009), who performed N-body simulation for different models (including models with cusp and models with two stellar disks); they concluded that the cusp could provide an additional heating of the stellar disk, leading to faster eccentricity/inclination growth.

Here we follow-up on the initial analytic work by Alexander et al. (2007), and extend it to include the role of a realistic detailed mass-function, the effects of stellar evolution, the impact of binary-heating and additional heating by a stellar cusp. This approach allows us to better understand and identify the role played by each of these processes and components, as well as to study the long-term evolution of realistic disks, which is more difficult (and computationally expensive) to study using full N-body simulations.

We begin by describing the dynamical processes that contribute to the stellar disk evolution, including stellar scattering, mass segregation and binary-heating (section 2). We then briefly review the structural components of the nuclear stellar cluster in which the disk is embedded, and consider various models for the mass function of the stellar disk, and the possible core-like or cuspy structure of the nuclear stellar cluster (NSC). The physical processes we consider as well as the NSC structural components are used to devise a multitude of possible models for the stellar disk evolution under diverse conditions, including considerations of stellar evolution (section 4). We present the results of the short and long term evolution of the disks considered in these models in section 5, and then discuss the results and their implications (section 6). We also briefly mention other possible physical processes not included in our current modeling. Finally we conclude and summarize our results in section 7.

2 THE DYNAMICS AND PHYSICAL PROCESSES IN A STELLAR DISK

In the following we briefly review several dynamical processes that contribute to the disk evolution. We first follow Alexander et al. (2007) in describing the two-body relaxation and mass-segregation (dynamical friction) of multiple stellar populations (extended to an arbitrary number of stellar populations), and then consider the analytic description of the effects of binary heating on stellar disks, not discussed before in this context.

2.1 Relaxation and single-star scattering

Let us follow Alexander et al. (2007) and consider a super massive black hole (MBH) with mass M_\bullet and N single stars with mass M orbiting the MBH in a initially thin stellar disk, with an external radius $R_0 + \Delta R/2$ and an internal radius $R_0 - \Delta R/2$.

When $M_\bullet \gg NM$ the relaxation time of such a system is given by Binney & Tremaine (2008).

$$t_{relax} = C \frac{\sigma^3}{G^2 M \rho \ln(\Lambda)} \quad (1)$$

With ρ the stellar density and $C \sim 1$ (depending only on the system geometry; e.g. for a spherical case $C \simeq 0.34$ (Binney & Tremaine 2008)). The disk density is given by

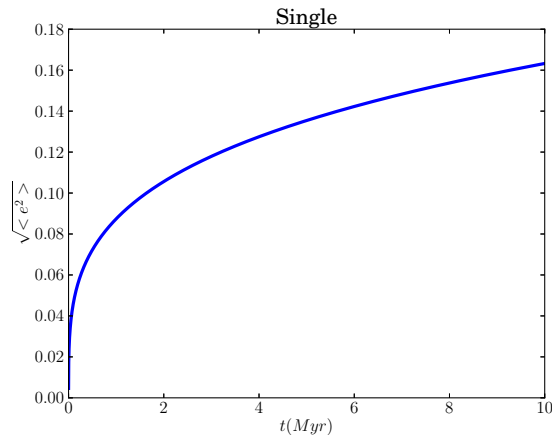


Figure 1. Evolution of the velocity dispersion of stars in a stellar disk composed of single mass stars orbiting a MBH; similar to Alexander et al. (2007).

$$\rho = \frac{NM}{2\pi R_0 H \Delta R}, \quad (2)$$

where $H = \sigma/\Omega$ is the scale height of the disk. We then obtain

$$t_{relax} = C \frac{R_0 2\Delta R \sigma^4}{G^2 N M^2 \ln(\Lambda)}. \quad (3)$$

Using this Eq. and defining $t_{orb} = 2\pi/\Omega$ we can describe the evolution of the velocity dispersion of disk stars:

$$\frac{d\sigma}{dt} = \frac{G^2 N M^2 \ln(\Lambda)}{C_1 t_{orb} R_0 \Delta R \sigma^3}, \quad (4)$$

with $C_1 = 2C$.

In a disk of stars orbiting an MBH, the root mean square (RMS) eccentricity of the stars can be related to their velocity dispersion by (Alexander et al. 2007, and references therein)

$$\langle e \rangle = e_{rms} = \sqrt{2} \frac{\sigma}{v_K},$$

where $v_K = (GM_\bullet/R_0)^{1/2}$ is the Keplerian orbital speed. The RMS inclination of stars is expected to be of the order of half the RMS eccentricity value. For comparison with observations of the eccentricities of stars in the Galactic center we therefore present our results of the RMS eccentricity (and inclination in some cases) rather than the velocity dispersion.

Fig. 1 shows the evolution of the RMS eccentricity of stars in the stellar disk, using a similar setup as used by Alexander et al. (2007)

2.2 Multi-mass components and mass segregation

Stellar scattering had also been considered for multi-mass stellar populations in the dispersion dominated regime (Alexander et al. 2007). In this regime, for two mass populations, Goldreich et al. (2004) suggest that the treatment of the problem only depends on the amplitude of the velocity dispersion (σ_2) of the lighter objects, with mass M_2 , compared with the Hill velocity of the more massive components, with mass M_1 . The Hill velocity for the more massive stars is defined as

$$v_{H,1} = \Omega R_{H,1}, \quad (5)$$

where $R_{H,1} = R_0(M_1/M_2)^{1/3}$. The dispersion dominated regime occurs when $\sigma_2 > v_{H,1}$. In this regime the speed of the single stars is similar to the velocity dispersion and scattering encounters are well approximated by two body dynamics. In the shear dominated regime, not discussed here, it is necessary to take into account the tidal gravity of the central black hole.

When the velocity dispersion of the low-mass stars satisfies $v_{esc,1} > \sigma_2 > v_{H,1}$, with $v_{esc,1}$ the escape velocity from massive stars, the exchange of momentum between the heavier and lighter bodies occurs through collisionless gravitational deflections, where gravitational focusing is important (Goldreich et al. 2004).

Considering only two stellar populations composed of N_1 and N_2 stars with stellar masses M_1 and M_2 , and velocity dispersions σ_1 and σ_2 , respectively, we obtain (Alexander et al. 2007):

$$\frac{d\sigma_1}{dt} = \frac{N_1 M_1^2}{A_1 t_{orb} \sigma_1^3} \ln(\Lambda_1) - \frac{N_2 M_1 M_2 \ln(\Lambda_{12})}{A_2 t_{orb}} \frac{\sigma_1}{\bar{\sigma}_{12}^4} \left(1 - \frac{E_2}{E_1}\right) \quad (6)$$

$$\frac{d\sigma_2}{dt} = \frac{N_2 M_2^2}{A_1 t_{orb} \sigma_1^3} \ln(\Lambda_2) - \frac{N_1 M_1 M_2 \ln(\Lambda_{12})}{A_2 t_{orb}} \frac{\sigma_2}{\bar{\sigma}_{12}^4} \left(1 - \frac{E_1}{E_2}\right), \quad (7)$$

where $\bar{\sigma}_{12} = (\sigma_1 + \sigma_2)/2$ and $A_i = (C_i R_0 \Delta R)/G^2$ for $i = 1$ and 2 , and $\Lambda_1 \Lambda_2$ are the appropriate Coulomb logarithms for the two stellar populations, which depend on the respective scale height of the disk. Λ_{12} is related to the scale height at which interactions between the two stellar species occur (see Alexander et al. 2007, for further details). The constant C_2 is related to the constant C_1 , and also depends on the geometry of the system. i.e for a three dimensional system $C_1/C_2 \simeq 3.5$ (for a detailed analysis please see at Stewart & Wetherill 1988); here we adopt the same value.

We can extend such a model to an arbitrary number of different stellar species, N . Each species adds an additional coupled equation and contributes a coupling term to each of the other equations. For the general case the time evolution of the velocity dispersions for each of the stellar species is given by a set of coupled equations

$$\frac{d\sigma_j}{dt} = \frac{N_j M_j^2}{A_1 t_{orb} \sigma_j^3} \ln(\Lambda_j) - \sum_{k \neq j} \frac{N_k M_j M_k \ln(\Lambda_{jk})}{A_2 t_{orb}} \frac{\sigma_j}{\bar{\sigma}_{jk}^4} \left(1 - \frac{E_k}{E_j}\right), \quad (8)$$

for $i = 1, 2, \dots, N$ and $k = 1, 2, \dots, N$ (with $k \neq j$).

From analyzing these set of equations we note that for two species, k and j for which $E_k > E_j$, the population of k -species particles dynamically heat the population of the j -species ones (leading to increased velocity dispersion) and vice versa (a less energetic population dynamically cools a more energetic one, dumping its velocity dispersion).

2.3 Interaction between the stellar disk and the nuclear cluster

The two-body relaxation of disk stars due to interaction with the background stars of the nuclear cluster can be modeled in a similar method to the two-body relaxation by different stellar populations discussed above. In this case, the cluster stellar population is considered as a distinct population with different properties. The disk

stars interact with those cluster stars which go through the disk, i.e if the volume of the disk is $V = 4\pi R_0 H \Delta R$, the number of cluster stars considered is the nuclear cluster stellar density times this volume. The velocity dispersion of this isotropic cluster population is $\sigma_{cluster} = V_K/\sqrt{3}$ (Binney & Tremaine 2008) with V_K the keplerian velocity around the MBH. We now use the same type of two-population interaction term in Eq. 8 to account for the effects of the cluster stars on the disk stellar population. Note that the cluster stellar population is much greater than the disk population, and can be assumed as a constant ‘‘heat’’ bath.

2.4 Binary Heating

Any stellar population is likely to contain some fraction of binary stars. An encounter between single stars and binaries could lead to an energy exchange between the binary orbital energy and the kinetic energy of the stars, i.e., energy can be exchanged between the inner degree of freedom of the binary and the outer external kinetic energy of the stars; thereby binaries can assist in dynamically heating the stellar disk.

Let us consider a binary system composed of stars with masses m_1 and m_2 , center of mass velocity V_{cm} , and orbital velocity V with respect to the center of mass of the system (we assume a circular binary for simplicity). The total energy of the binary can be expressed as (Binney & Tremaine 2008):

$$E = \frac{1}{2}\mu V^2 - G \frac{m_1 m_2}{r} + \frac{m_1 + m_2}{2} V_{cm}^2,$$

where $\mu = \frac{m_1 m_2}{m_1 + m_2}$ is the reduced mass. The sum of the first two left element define the binding energy, E_b , in terms of the semi-major axis

$$E_b = -G \frac{m_1 m_2}{2a}. \quad (9)$$

Binary-single encounters had been explored extensively, with the pioneering studies by Heggie (1975) and Hills (1975). Binaries can be divided into two dynamical categories; ‘‘Hard Binaries’’ and ‘‘Soft Binaries’’: when the kinetic energy of the intruding mass, E_k , is such that $E_k/m_b V^2 \ll 1$, (where $m_b = m_1 + m_2$ is the binary total mass) a binary is considered to be hard (where the lower the ratio the harder the binary); it is considered to be a soft binary when $E_k/m_b V^2 \gg 1$.

Heggie (1975) and Hills (1975) found that following a binary-single encounter soft binaries become softer and hard binaries become harder (on average), a behavior typical termed as ‘‘Heggie’s law’’.

The long term typical evolution of a binary randomly encountering stars in some dense environment can then be modeled using a simple approach. Considering a binary in a field of incoming stars with typical mass m and particle density n , the averaged evolution of the binding energy of the binary due to many encounters is given by

$$\left\langle \frac{dE_b}{dt} \right\rangle = n \langle \sigma_E V \rangle E_b, \quad (10)$$

where V the typical relative velocity of the intruders, and σ_E the cross section of the single-binary collisions. We may now consider the contribution of a stellar population i with stellar density n_i which is composed of stars with typical mass m_i , to the bi-

nary evolution; when the velocity distribution of incoming stars is Maxwellian and taking Eq. 10 can be expressed as (Hills 1992):

$$\left\langle \frac{dE_b}{dt} \right\rangle = \frac{\sigma_E^* (6\pi)^{\frac{1}{2}} G^2 m_b^2 \rho_i}{4\sqrt{\langle V_i^2 \rangle}} \left(\frac{m_i + m_b}{m_b} \right)^{1.2} \left(\frac{1}{2\frac{m_i}{m_b} + \frac{1}{3}} \right), \quad (11)$$

where $m_b = m_1 + m_2$, $\rho_i = n_i m_i$. Hills (1992) made use of N-Body simulations to study the dependence of σ_E^* on the intruder mass (m_i) and the binary mass (m_b) in the mass-ratio range $2m_i/m_b \in [0.01, 10000]$ and found that the empirical functional dependence can be formulated by

$$\sigma_E^* = \frac{a + cx + ex^2 + gx^3}{1 + bx + dx^2 + fx^3}$$

with $x = \ln(2m_i/m_b)$, $a = 1.26$, $b = -0.15$, $c = 0.054$, $d = 0.02$, $e = 0.1$, $f = 0.0045$ and $g = 0.015$.

For a single star the average kinetic energy is $\langle E \rangle = 3m\sigma_i^2/2$ with σ_i the velocity dispersion. Taking $\sigma_i \sim \sqrt{\langle V_i^2 \rangle}$ (encounter velocity \sim dispersion velocity) and applying energy conservation for a system of binary stars with density n_b we get

$$n_i \left\langle \frac{dE}{dt} \right\rangle = -n_b \left\langle \frac{dE_b}{dt} \right\rangle. \quad (12)$$

Eqs. 11 and 12 give

$$\frac{d\sigma_i}{dt} = D_i \frac{n_b}{3n_i m_i \sigma_i^2} \quad (13)$$

with

$$D_i = \frac{\sigma_E^* (6\pi)^{\frac{1}{2}} G^2 m_b^2 \rho_i}{4} \left(\frac{m_i + m_b}{m_b} \right)^{1.2} \left(\frac{1}{2\frac{m_i}{m_b} + \frac{1}{3}} \right). \quad (14)$$

We can now use Eq. 13 as the binary-heating term to be added to the dynamical evolution equation for the stellar disk populations (Eq. 4); allowing us to model the binary-heating contribution.

We are now in a position to assess whether binary heating can play an important role in heating the stellar disk. For the simplest case of a disk with only one population of same-mass stars and a binary fraction n_b , the velocity dispersion evolution equation is obtained by summing the scattering term and the binary heating to get (taking $m_b = m_i = M$)

$$\frac{d\sigma}{dt} = \frac{G^2 N M^2 \ln(\Lambda)}{C_1 t_{orb} R_0 \Delta R \sigma^3} + D_i \frac{n_b}{3n_i M \sigma^2},$$

or after some math

$$\frac{d\sigma}{dt} = \frac{G^2 N M^2}{t_{orb} R_0 \Delta R \sigma^3} \left[\frac{\ln(\Lambda)}{C_1} + \frac{N_b}{N} K \right], \quad (15)$$

where N_b is the number of binary stars, and

$$K = \frac{\sigma_E^* (6\pi)^{\frac{1}{2}} 2^{-0.8}}{7} \simeq 0.53.$$

We can now compare the relative contribution by single-star scattering and binary heating through the comparison of the two terms in Eq. 15. If we consider some typical initial conditions in the Galactic center, taking $\ln(\Lambda) \simeq 7.5$ (as the disk heats-up the

scale height grows but with only a small corresponding change in $\ln(\Lambda)$ due to the logarithmic dependence), $C_1 \simeq 3$ and a binary fraction of $2/3$, $N_b = (2/3)N$, we find that the relative contribution of binary heating is only one tenth of the contribution due to single star scattering. This can be seen explicitly in the evolution of the velocity dispersion shown in Fig. 2. The left panel shows how the exclusion of the binary heating contribution (for a disk in which $M_{single} = M_{binary} = 20M_\odot$) makes only a very small difference (see also the effect of accounting only for binary heating). We can therefore conclude that although the binaries binding energy could be larger than the kinetic energy of the disk, the rate of extraction of this energy and its exchange into the disk kinetic energy is negligible, at least for the relatively thin disks considered here.

2.5 Full model

We can combine the stellar disk contributions described above to obtain the full set of equations describing our model, including multi-mass populations, binaries and nuclear cluster stellar population. This is summarized below;

$$\begin{aligned} \frac{d\sigma_j}{dt} = & \frac{N_j M_j^2}{A_1 t_{orb} \sigma_j^3} \ln(\Lambda_j) \\ & - \sum_{k \neq j} \frac{N_k M_j M_k \ln(\Lambda_{jk})}{A_2 t_{orb}} \frac{\sigma_j}{\sigma_{jk}^4} \left(1 - \frac{E_k}{E_j} \right) \\ & + \sum_i D_{ij} \frac{n_{binary-i}}{3n_j M_j \sigma_j^2} \\ & - \sum_i \frac{N_{binary-i} M_j m_{binary-i} \ln(\Lambda_{j-binary-i})}{A_2 t_{orb}} \\ & \frac{\sigma_j}{\sigma_{j-binary-i}^4} \left(1 - \frac{E_{binary-i}}{E_j} \right) \\ & - \frac{N_{cusp} M_j M_{cusp} \ln(\Lambda_{j-cusp})}{A_2 t_{orb}} \frac{\sigma_j}{\sigma_{j-cusp}^4} \left(1 - \frac{E_{cusp}}{E_j} \right) \end{aligned} \quad (16)$$

where

- (i) $\Lambda_{j-cusp} = \bar{\sigma}_{j-cusp} \Delta R / 2GM_\odot$
- (ii) $\bar{\sigma}_{j-cusp} = (\sigma_{cusp} + \sigma_j) / 2$,
- (iii) $\sigma_{cusp} = \frac{1}{3} \sqrt{GM_T(R) / R}$
- (iv) $M_T(R) = M_{cusp}(R) + M_{SMBH}$
- (v) $M_{cusp}(R) = \int_{R_{min}}^{R_{max}} 4\pi r^2 \rho_{cusp}(r) dr$, where we consider the effective region to affect the stars to be between $R_{min} = 0.5R$ and $R_{max} = 1.5R$ and
- (vi) $\rho_{cusp}(r) \propto r^{-\gamma}$
- (vii) $\Lambda_{j-binary-i} = \frac{(\sigma_j + V_{i-orbital})^2}{2GM_{binary-i}}$, where $V_{i-orbital}^2 = \frac{GM_{binary-i}}{a_i}$ and a_i is semi-major axis of the binary.
- (viii) $\Lambda_{jk} = \frac{\sigma_{jk} \Delta R}{2GM_k}$

3 STRUCTURAL COMPONENTS OF THE NUCLEAR STELLAR CLUSTER

In the following we describe the observed properties of the cluster and the embedded stellar disk, and the models we use in our analysis.

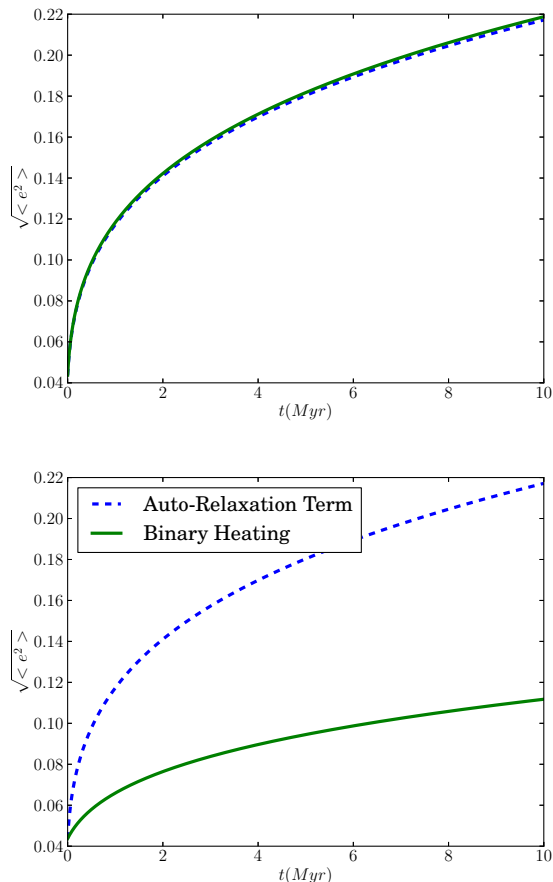


Figure 2. Evolution of RMS eccentricity for model X (in Section 4 and Table 3 for more information about the models). In the top panel is plotted the evolution of RMS eccentricity through time, the dashed line is the model only considering auto-relaxation and the solid one is when binary heating is included. In the bottom panel are plotted the evolution of the RMS eccentricity when only auto-relaxation (dashed line) or binary heating is considered (solid line).

3.1 Observed disk structure and mass function

Beginning with the analysis of Levin & Beloborodov (2003), observations have shown the existence of a young stellar disk near the MBH in the Galactic center. Paumard et al. (2006) showed that many of the observed young O/WR/B-stars reside in a disk-like structure between $\sim 0.05 - 0.5$ pc from the MBH.

Early measurements suggested the disk-stars revolve around the MBH in somewhat eccentric orbits. Bartko et al. (2009) found an RMS eccentricity of $\langle e \rangle = 0.37 \pm 0.07$ for the disk stars, but the most recent studies suggest a smaller value of $\langle e \rangle = 0.27 \pm 0.07$ (Yelda et al. 2014). The disk-stars appear to be young, forming only 4 – 7 Myrs ago (Paumard et al. 2006). The radial surface density profile of the disk can be described by a power-law distribution, $\Sigma(R) \sim R^{-\beta}$, with β in the range [1.5, 2.3] (Paumard et al. 2006; Lu et al. 2009; Bartko et al. 2009, 2010).

Initially it was thought that $\sim 40 - 50\%$ of the young stars belong in the disk structure; however, more recent studies suggest that only $\sim 20\%$ of these reside in the disk, while most of the stars have more spherical distribution, outside the disk (Lu et al. 2009). Here we consider only the evolution of disk stars.

In most galactic environments the initial mass function (IMF)

describes the distribution of stellar masses at birth. Analysis of observations (Salpeter 1955, Chabrier 2001, Kroupa 2002) shows an almost universal power law behavior, with $dN(m) \propto m^{-\alpha(m)} dm$, with a typical exponent of $\alpha \sim 2.3$, for stars above one Solar mass and up to $\sim 120 M_{\odot}$. The analysis done by Bartko et al. (2010) based on spectroscopic survey made with SINFONI conclude that the present day mass function and the IMF for the disk of young stars in the Galactic center obey a power law, but the slope is flatter than the “regular” IMF. In particular, they conclude that $\alpha = 0.45 \pm 0.3$. In such a “top heavy” IMF, massive stars are much more frequent compared with the Salpeter IMF.

3.2 Disk models

In our models we consider an initially thin cool disk ($H \ll \Delta R$ and low initial eccentricities for the star, i.e. we assume an initially low velocity dispersion for the disk stars) rotating at angular speed $\Omega = V_K/R_0$ (with V_K the Keplerian velocity).

We only consider the evolution of the disk stars and do not discuss the origin and evolution of the more spherical component of the young stars in the Galactic center.

We studied three different types of disks: a single-mass disk, an Initial Mass Function (IMF) disk and disk with binaries.

3.2.1 Mass function

We consider various mass functions for the stars in the stellar disk and the cusp. These different models are summarized in the following.

Single-mass model: In the simplest, unrealistic model studied here, we consider a stellar disk composed of single-mass stars, similar to the basic models considered by Alexander et al. (2007), as a test-case for comparison.

Top-heavy initial mass-function model: In this model we assume the initial mass function of the disk stars is a top-heavy mass function with masses in the range $0.6 - 120 M_{\odot}$, as suggested by Bartko et al. (2010, see discussion above).

Salpeter mass function: In this case we assume the initial mass function of the stars in the stellar disk is a Salpeter mass function with masses in the range $0.6 - 120 M_{\odot}$.

3.2.2 Binarity

Our knowledge about binaries in the GC is currently limited, but Observation by Ott et al. 1999 and Martins et al. 2006 show the existence of at least some young binaries in the Galactic center. In particular, they found that one of the brightest O/WR star in the GC is a massive binary star ($M_b \sim 100 M_{\odot}$). More recent works (Rafelski et al. 2007) found a few additional binary O-star candidates, though no binaries had been found among the young B-stars. These studies either rely on detection of eclipsing binaries or through radial velocity detection of short-period binaries, and are therefore mostly sensitive to close binaries. It is therefore difficult to estimate the underlying binary fraction among the young stars in the Galactic center using these limited statistics. Taking them at face value would suggest a very high binary fraction, comparable or even larger than the high binary fraction observed in the field for similarly young massive stars (Sana et al. 2012).

On the theoretical side, most binaries in the Galactic center are expected to be “soft” binaries and therefore have relatively short lifetime due to perturbations by other stars (Bahcall & Wolf 1977; Ozernoi & Dokuchaev 1982; Hopman 2009; Perets 2009a; Alexander & Pfuhl 2014), or merge due to secular perturbations by the massive black hole (Perets 2009b; Antonini & Perets 2012; Prodan et al. 2015). The binary fraction among the old stellar population in the nuclear cluster is likely to be negligible, and we do not include it in any of our calculations.

Binaries in the disk could, however, be “hard” in respect to the other disk stars, given the low-velocity dispersion in the disk. The young age of the disk also suggests that most of the initially formed binaries should still survive. Overall it is therefore likely that the binary fraction of the massive stars in the Galactic center stellar disk is high as in the field ($> 50\%$), and that the binary fraction does not evolve much since its formation.

As we discussed above, binaries are generally not very important for the disk evolution, but we do consider them in some of our models for completeness, in which case we assume a binary fraction of 50%.

3.3 Cusp and core models for the nuclear cluster

A stellar cluster around a massive black hole is expected to evolve into a stellar cusp structure over a relaxation time (Bahcall & Wolf 1976, 1977). For a spherically symmetric distribution of equal-mass stars analytic considerations and N-body simulations show that in equilibrium the density profile of the cluster has a power-law distribution, $\rho \propto r^{-\gamma}$, with $\gamma = 7/4$ (Bahcall & Wolf 1976). Mass segregation in multi-mass clusters produce mass-dependent density profiles for the different mass stellar populations, with $\rho(m) \propto r^{-\gamma(m)}$, where $\gamma(m) = 1.5 + m/(4m_{\max})$, with m_{\max} the mass of the heaviest stellar element (Bahcall & Wolf 1977).

Hopman & Alexander (2006b) used Fokker-planck calculations to show that γ should be 1.4 for solar mass MS stars and up to 2 for stellar black holes (SBH). Similar results from Monte-Carlo calculations were found by Freitag et al. (2006) However, observations of red-giants in the Galactic center suggest a core-like structure in the inner regions of the GC (γ in the range 0 – 0.5; Do et al. 2009; Bartko et al. 2010; Genzel et al. 2010. Nevertheless, it is not yet clear whether the distribution of red-giants reflect the overall distribution of stars in the GC, and various models had been suggested to explain both a “real” core distribution (Merritt 2010) or an apparent one (i.e., only reflecting the distribution of red-giants; Dale et al. 2009; Amaro-Seoane & Chen 2014; Aharon & Perets 2015).

In light of the above discussion, we consider two possible models: (1) A cusp model dominated by a steep power-law distribution of SBHs ($\gamma = 2$) and (2) A core model with a shallow power-law distribution ($\gamma = 0.5$).

3.4 Stellar evolution and the long term evolution of disks

In addition to our study of the role of the different NSC and disk components, we also considered the effects of stellar evolution, which become especially important once the long term evolution of the stellar disk is explored. We considered the evolution of disks with various properties (see below) both at times comparable to the observed stellar disk in the GC (up to 10 Myrs), as well as a longer term (100 Myrs) evolution.

Table 1. The final mass and final type after T_{MS} (of each star) for different intervals of mass. However star with initial mass less than $6.5M_{\odot}$ has T_{MS} greater than 100Myr.

Initial Mass [M_{\odot}]	Final remnant mass (after T_{MS})[M_{\odot}]	Type of remnant
$30 < M \leq 120$	10	SBH
$15 < M \leq 30$	7	SBH
$8 \leq M \leq 15$	1.4	NS
$6 \leq M \leq 8$	1	WD

Table 2. NSC Models.

Model	Star	$M (M_{\odot})$	γ	$\rho_0 (M_{\odot} \text{pc}^{-3})$
CUSP I	MS	1	2.0	5.2×10^5
CUSP II	MS	1	1.4	1.9×10^6
	SBH	10	2.0	1.8×10^5
CORE	MS	1	0.5	5.2×10^5

We first considered simple models in which we did not introduce any stellar evolution, and assumed stars do not change over time. We then consider the effects of stellar evolution in a simplified manner. For each stellar population in a given mass-bin we consider the appropriate MS lifetime for a star of such mass, T_{MS} , according to stellar evolutionary models. After that period we replace the star in the model with the stellar remnant it produces, assuming a simplified prescription as described in table 1; in particular the continuous mass-loss process is simplified and the mass loss is assumed to be immediate. We only considered evolution of up to 100 Myrs and hence we do not consider the stellar evolution of stars with masses smaller than $6 M_{\odot}$.

4 DETAILED MODELS

In the following we describe the specific evolutionary models we discuss in detail. We consider a disk of stars orbiting a MBH with mass $M_{\bullet} = 4 \times 10^6 M_{\odot}$. The inner disk radius is $R_{in} = 0.05 \text{pc}$, and the external radius $R_{out} = 0.15 \text{pc}$ (so $\Delta R = 0.1 \text{pc}$). The initial velocity dispersion is assumed to be low (i.e. a cool thin disk with low eccentricity orbits) (initial velocity dispersion $\sigma_{j0} \ll V_K$ for any disk population j ; we take than $\sigma_{j0} = 0.03V_K$). We take a disk surface density of $\Sigma(R) \propto R^{-1}$ (following similar assumptions as Cuadra et al. 2008 and Prodan et al. 2015).

We consider several models for the nuclear cluster, both cusp and core models. We study two different cusp models. The CUSP I model is composed of single, solar mass stars (see Prodan et al. 2015, for details) with a density profile profile

$$\rho(r) = \rho_0 \left(\frac{r}{r_0}\right)^{-\gamma} \left[1 + \left(\frac{r}{r_0}\right)^2\right]^{\frac{(\gamma-1.8)}{2}}, \quad (17)$$

with $r_0 = 0.5 \text{pc}$, $\rho_0 = 5.2 \times 10^5 M_{\odot} \text{pc}^{-3}$ and $\gamma = 2$.

The CUSP II model is a multi-component cusp, with two populations; MS stars of $1 M_{\odot}$, and SBHs of $10 M_{\odot}$. These have a power-law $\rho \propto r^{-\gamma}$, distributions with $\gamma_{MS} = 1.4$ $\gamma_{SBH} = 2$, respectively; following the results of Hopman & Alexander (2006b). Finally the CORE model is similar to CUSP I model but with $\gamma = 0.5$. The models properties, are summarized in Table 2.

We studied different models for various disk and cluster combinations. A brief summary of the properties of the models is given in Table 3, including the disk mass function and its binary fraction.

Table 3. Summary of the properties of the disk and nuclear cluster models, including their mass functions and density profiles.

#	Disk	Cusp/Core	Masses in the cusp	γ	M_{\min}	M_{\max}	Γ	Binary fraction
I	O-stars with $M_* = 20M_{\odot}$	-	-	-	-	-	-	-
II	O-stars with $M_* = 20M_{\odot}$	CUSP I	$1M_{\odot}$ MS stars	1.5	-	-	-	-
III	O-stars with $M_* = 20M_{\odot}$	CORE	$1M_{\odot}$ MS stars	0.5	-	-	-	-
IV	Salpeter IMF	-	-	-	$0.6M_{\odot}$	$120M_{\odot}$	2.35	-
V	Salpeter IMF	CUSP I	$1M_{\odot}$ MS stars	1.5	$0.6M_{\odot}$	$120M_{\odot}$	2.35	-
VI	Salpeter IMF	CORE	$1M_{\odot}$ MS stars	0.5	$0.6M_{\odot}$	$120M_{\odot}$	2.35	-
VII	Top-Heavy IMF	-	-	-	$0.6M_{\odot}$	$120M_{\odot}$	0.45	-
VIII	Top-Heavy IMF	CUSP I	$1M_{\odot}$ MS stars	1.5	$0.6M_{\odot}$	$120M_{\odot}$	0.45	-
IX	Top-Heavy IMF	CORE	$1M_{\odot}$ MS stars	0.5	$0.6M_{\odot}$	$120M_{\odot}$	0.45	-
X	O-stars with $M_* = 20M_{\odot}$	-	-	-	-	-	-	0.4
XI	O-stars with $M_* = 20M_{\odot}$	CUSP II	$1M_{\odot}$ MS / $10M_{\odot}$ SBH	1.4/ 2.0	-	-	-	-

5 RESULTS

In the following we present the evolution of stellar disks for the different models considered. We first study simpler cases with single-mass disks and then progressively consider more and more realistic cases. These include disks composed of stars with a range of masses and different mass-functions, and the effects of different types of NSCs. In this case we also explore the differential evolution of stars of different masses in the same disk and their stratification. We then consider the effects of stellar evolution on the disk, and the long term (100 Myrs) evolution of stellar disks.

5.1 Evolution of Single-mass disks

Fig. 3 shows the evolution of the RMS eccentricity of the disk stars for disks with single-mass stars (models I, II, III and XI), for different choices of mass (10 and $20M_{\odot}$ stars). As expected the cusp heating has a stronger effect on lower mass stars.

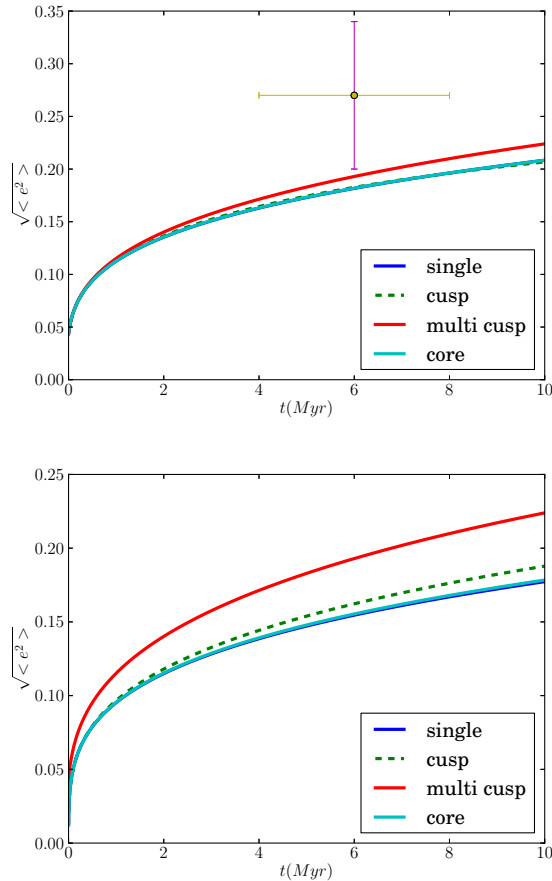
5.2 Dependence on stellar mass and the structure of the nuclear stellar cluster

Fig. 4 shows the role of the cusp and its structure on the evolution of disk stars, and the role of the single-star masses. The final RMS eccentricity (after 10Myr) is shown for a range of single-mass disks (models I, II and III). Each point in the lines corresponds to a disk with the same total mass, but the mass of the stars composing the disk, indicated on the X-axis (same for all stars in the disk) differs. Disks composed of lighter stars can be seen to be more sensitive to the heating by NSC stars, with the cusp model being more effective than the core one. In contrast, disks composed of heavy stars are cooled down by the NSC (compared with the model with no existing NSC).

5.3 Multi-component NSCs

In the previous section we studied the evolution of stellar disks and their interaction with single-mass NSC stellar population. In the following we consider a more complex and potentially more realistic model for the NSC. In our multi-component NSC we follow model XI, where the NSC includes both SBHs and MS solar mass stars. Fig. 5 shows the disk evolution in such model. Though the number of SBHs in the cusp is relatively small, they can play an important role in heating a disk of massive $20M_{\odot}$ stars, where more massive SBHs lead to stronger heating of the disk.

Fig. 6 shows that the inclusion of SBHs in addition to Solar


Figure 3. Evolution of RMS eccentricity of single-mass disk stars. Upper panel shows models I, II, III and XI. Bottom panel shows evolution of similar models but with disk stars mass of $10M_{\odot}$. Also shown are the measured RMS eccentricity of the O-stars in the GC disk (Yelda et al. 2014).

mass stars in the cusp (model XI) leads to a more prominent disk heating, as expected.

5.4 Evolution of multi-mass disks

In models IV – IX we studied the evolution of multi-mass stellar populations in a disk, where we considered both disks with Salpeter IMFs as well as disks with top-heavy IMFs. For each model we divided the masses into 20 logarithmic mass bins for the Salpeter

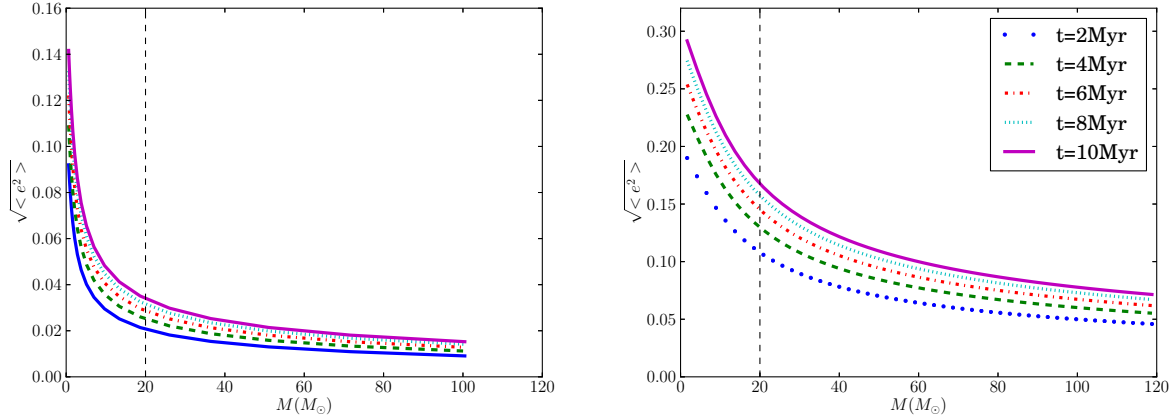


Figure 7. Evolution of the RMS eccentricity of stars with different masses in the same disk. The upper panel corresponds to a disk with a Canonical IMF (Salpeter, $\Gamma = 2.35$) and the bottom one corresponds to a disk with a top-heavy IMF ($\Gamma = 0.45$). The different lines, ordered from bottom to top correspond to the evolutionary times: 2, 4, 6, 8 and 10 Myrs, respectively.

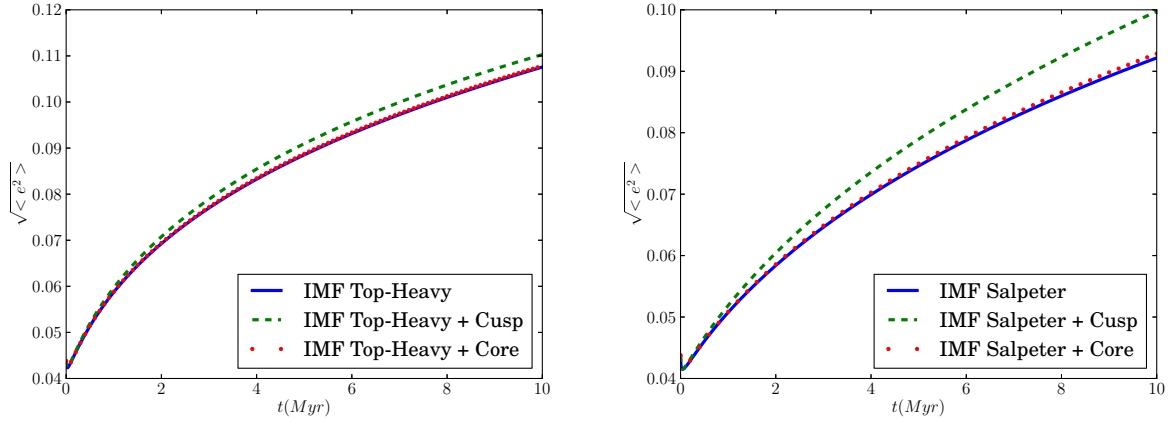


Figure 8. Evolution of the RMS eccentricity of all stars (of any mass) in each of the models. The left panel shows top-heavy IMF ($\Gamma = 0.45$) models and the right one shows models with a Salpeter IMF ($\Gamma = 2.35$). Solid lines correspond to models without any NSC contribution.

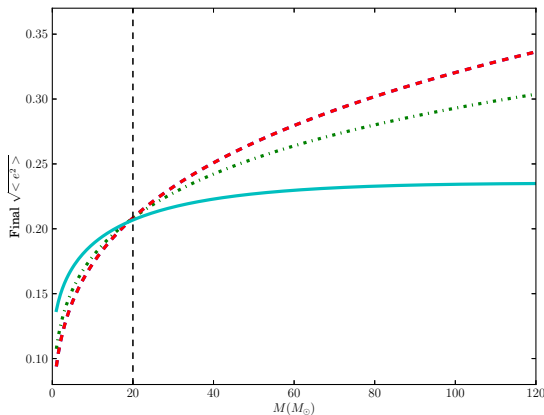


Figure 4. The RMS eccentricity of disk stars after 10 Myr of evolution. The solid line corresponds to Model II, dot-dashed is for core Model III, and the dashed line corresponds to the case where no NSC exists.

IMF cases; for better mass resolution we considered linear mass bins for the Top-Heavy IMF. For each mass bin we add a coupled equation (8), where we took the mass weighted average to represent the mass bin, with the appropriate number of stars in that mass bin.

Fig. 7 shows that the disk evolution leads to a mass stratified structure of the disk, with lighter stellar populations being excited to higher eccentricities/inclinations (and larger scale height for their disk component) compared with populations of more massive stars, which are segregated to more circular orbits in the central part of the disk (lower scale height). Such stratification is also observed for models including the effect of the NSC, where only small differences exist as a function of the stellar masses; lower mass stars are more sensitive to the NSC heating (not shown), as expected.

The top-heavy IMF models include a significantly larger number of more massive stars, leading to a much faster heating of the stellar disk, as also observed in the simple models considered by Alexander et al. (2007). As can be seen in Fig. 8, the NSC can further contribute to the disk heating, leading to $\sim 10\%$ higher RMS eccentricity, but its contribution becomes negligible in the top-heavy IMF cases, where the heating is dominated by the massive stars in the disk.

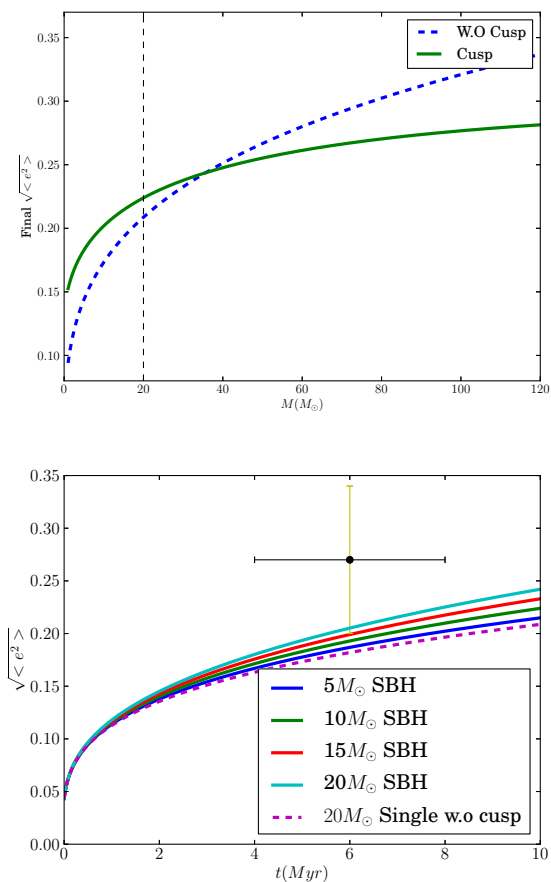


Figure 5. Evolution of a stellar disk composed of $20 M_\odot$ stars, embedded in a multi-component cuspy NSC (model XI). The left panels shows the comparison between the disk+multi-component cusp model and a model without an NSC component. The right panel shows the evolution of a disk embedded in cuspy NSCs, where different masses for the NSC SBH population are considered. Also shown are the measured RMS eccentricity of the GC O-stars (Yelda et al. 2014).

In order to compare these results with the measured RMS eccentricity of the O-stars in the GC we now consider only the RMS eccentricity of $3\text{--}40 M_\odot$ stars, more comparable to the O/B stars observed in the disk today. For an age of $5\text{--}7$ Myrs for the GC stellar disk we expect an RMS eccentricity of the order of 0.14, significantly lower than the measured $\langle e \rangle = 0.27 \pm 0.07$ (Yelda et al. 2014).

5.5 Stellar evolution and the long term evolution of stellar disks

Fig. 10 shows the long term (100 Myr) evolution of the stellar populations in disks with continuous (Salpeter or top heavy) IMFs, where simplified stellar evolutionary mass loss is considered (see section 3.4).

As each of the modeled disks evolve, progressively more massive stars end their life and become lower mass stellar remnants. These (now) lower-mass remnants can then be heated much more effectively through mass-segregation processes. Once the more massive stars evolve the role of the cusp heating becomes more significant, as be seen from the comparison between the no-NSC

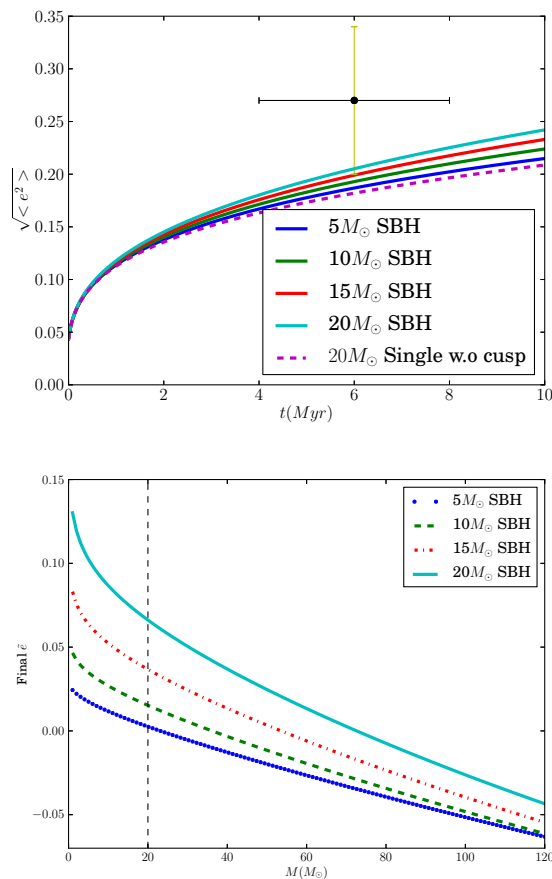


Figure 6. Evolution of RMS eccentricity for a disk of O-Stars with multi-component cusp (model XI), each color is for different SBH mass. The dashed line is to compare to model I. On the left panel is plotted the evolution through the time. The right panel is the difference between the final eccentricity for each model compared to model I.

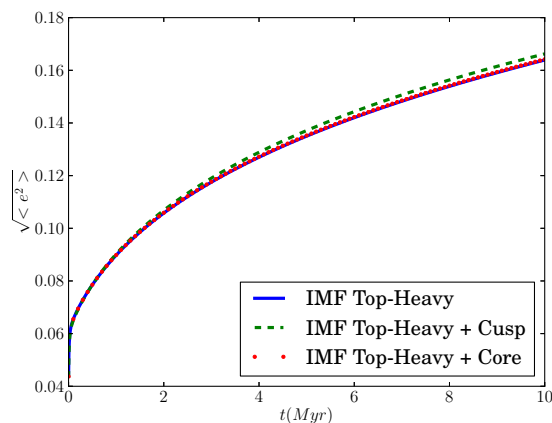


Figure 9. Evolution of the RMS eccentricity of stars in the mass range $3M_\odot < M < 40M_\odot$ corresponding to OB stars currently observed in the GC disk.

and cuspy NSC models. Moreover, with the absence of high mass stars intermediate mass populations begin to cool, when no cusp exists; but these same populations continue to heat up when a cusp population do exist.

6 DISCUSSION

In this work we studied the evolution of a stellar disk around a MBH. We followed previous analytic models developed by Alexander et al. (2007), which considered two-body relaxation and mass segregation processes, and extended the models to include the effect of binary heating, and role of the nuclear cluster interactions with the disk, using several plausible models for the NSC. We also studied realistic mass function models for the disk stellar populations, and included simplified models for the stellar evolution of the stars. Finally, we also explored the long term (100 Myrs) evolution of such disks. In the following we discuss our results and their implications for the role played by the different processes and components in sculpting the disk evolution.

6.1 Disk heating and mass stratification

Similar to the results of Alexander et al. (2007), we confirm that for isolated stellar disks, the disk heating is dominated by dynamical friction /mass-segregation processes in which the more massive stars heat the low mass stars. Correspondingly, the more massive stars are cooled by the interaction with the low-mass stars, but two-body relaxation of the massive stars by themselves still keeps heating them. Models with top-heavy mass function include a larger fraction of massive stars, and therefore allow for more rapid heating of the disk, producing larger RMS eccentricities.

Our models considered detailed mass-functions for the stars in the disk, allowing us to estimate the evolution of different stellar populations. As seen in Fig. 7, the disks develop mass stratification where higher mass stellar populations are expected to have significantly lower disk height scale and more circular orbits compared with the low mass stars in the disk. The existence, or lack of such mass stratification in the GC stellar disk could therefore be an important tool in assessing the processes involved in the evolution of the GC disk and its initial conditions.

6.2 The role of the cusp

The effect of the NSC on the evolution of the stellar disk was not considered before in analytic models. The NSC stellar population has a high velocity dispersion, i.e. it is an effectively “hotter” population than the “cool” stellar disk population. The NSC can therefore potentially heat the stellar disk, even when it is composed of low-mass stars.

Our results suggest that a dense cuspy NSC can play a non-negligible, though limited role in heating the stellar disk. When the disk contains a large population of massive stars, these dominate the disk heating and evolution, and the NSC plays a relatively minor role. Nevertheless, even young disks in which massive stars still exist are affected by the NSC, with top-heavy IMF disks being relatively little affected, but Salpeter-IMF disks showing non-negligible heating up to $\sim 10\%$ higher RMS eccentricities.

The NSC effects are more prominent in cases where the disk is dominated by low mass stars. These include unrealistic cases of disks composed of low single-mass stars, but they also relevant for the long term evolution of stellar disks with realistic IMFs. In the

latter case stellar evolution leads to the transformation of massive stars into low mass stellar remnants over time. The effective mass-function of such evolving stellar disks therefore becomes progressively centered around lower mass stars and stellar remnants which replace the previously existing massive stars. Correspondingly, the NSC heating of the cusp plays a progressively more dominant role in the disk evolution as can be seen in Fig. 10.

6.3 The role of binary heating

In this study we extended the analytic study of stellar disk evolution to include binary heating processes. In principle the binding energy stored in binaries is significant; however, the rate of energy exchange between the binaries and the single stars in the disk is slow. Therefore, binary heating is inefficient in heating the stellar disk, compared with two-body relaxation and mass-segregation processes. These results are consistent with N-body simulation results which included binaries done by Cuadra et al. (2008).

Note that we consider the overall averaged evolution of the stellar disk population; atypical single-binary encounters with short-period massive binaries can lead to strong kicks ejecting stars at high velocities, even beyond the escape velocity from the NSC (Perets & Šubr 2012). Such encounters may produce a small number of outlying stars at highly eccentric/inclined orbits, but are not likely to significantly affect the overall evolution of the disk and its averaged properties (see also Perets et al. 2008).

6.4 The long term evolution of stellar disks and their signature

We find that the disk evolution over times as long as 100 Myrs is slow. Two-body relaxation is too inefficient for the disk to assimilate into the nuclear cluster on such timescales. The disk structure is expected to keep its coherency, and be observed as a relatively thin disk even at 100 Myrs. This suggests that the existence of older disks formed before the one currently observed in the GC might still be inferred from the stellar kinematics of older, lower mass stars, which may still show a disk-like structure, unless destroyed/smeared by other non-two-body relaxation processes.

6.5 Other physical processes (and caveats)

Our analytic approach considered the role of two-body relaxation and binary heating, and included realistic disk and NSC components. However, secular processes and possible collective effects are beyond the scope of such a model; we briefly review studies of these processes.

Resonant relaxation processes (Rauch & Tremaine 1996) could potentially lead to fast evolution of disk stars inclinations through the vector resonant relaxation (and slower evolution of the eccentricities), especially in the inner parts of the disk (Hopman & Alexander 2006a). Kocsis & Tremaine (2011) suggested that resonant relaxation can produce significant effects, however they assumed an unrealistic effective mass of NSC stars, which is 5-10 times larger than expected in the GC (even when including stellar black holes). Further study of this effect under realistic conditions could shed more light on this issue.

Fast two-body relaxation as well as secular evolution of disk stars could also be induced by massive coherent components, massive perturbers (Perets et al. 2007) such as molecular

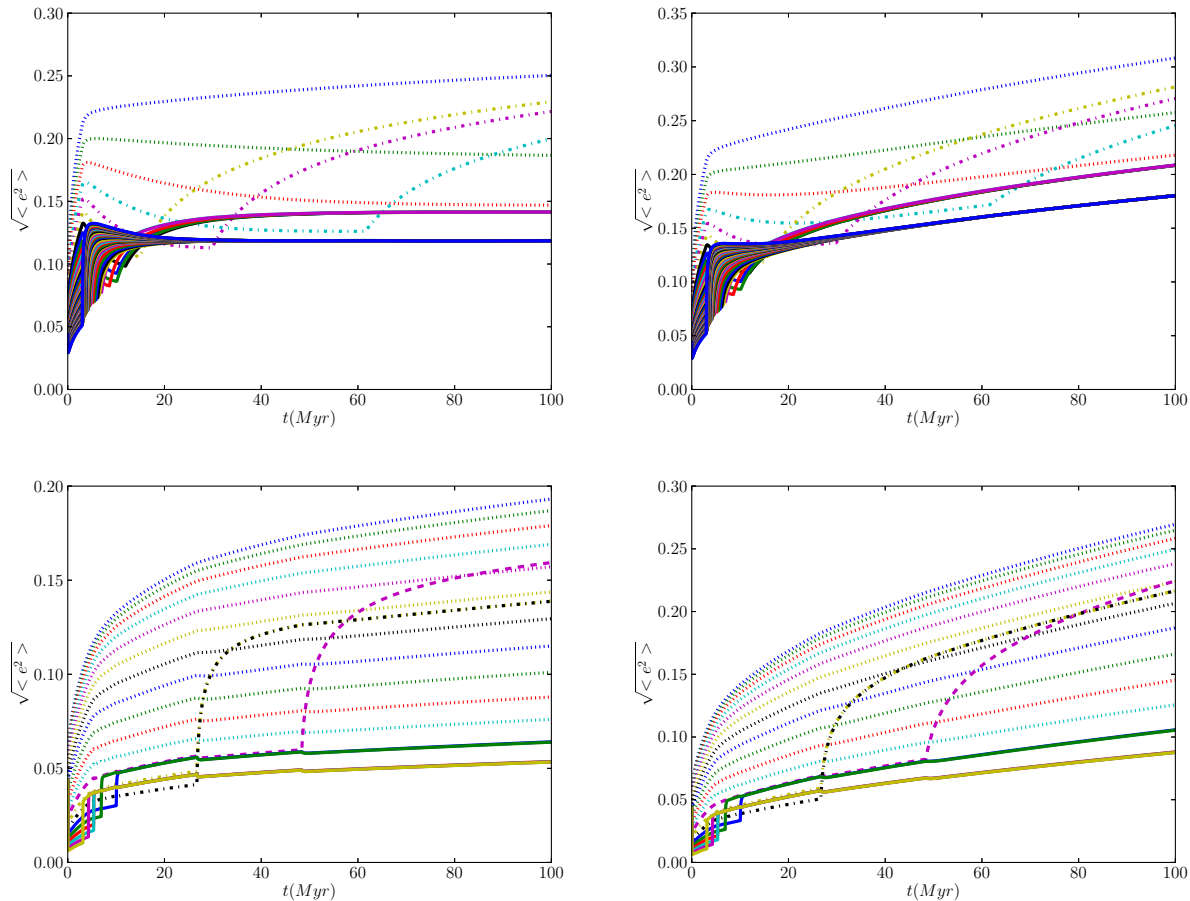


Figure 10. The long term evolution of the RMS eccentricity of disk stars in over 100 Myrs. Simplified stellar evolution is included (see main text). Top panels show the evolution of a disk with a Top-Heavy IMF ($\Gamma = 0.45$). Bottom panels show the evolution of a disk with a Salpeter IMF ($\Gamma = 0.45$). The left and right panels correspond to models without an NSC and with a cuspy NSC, respectively. The lines from bottom to top (initially) correspond to increasingly less massive stars. The solid, dashed, dashed-dotted and dotted lines correspond to star that evolve to become SBHs, NSs, WDs or MSs, respectively.

clouds, stellar clusters, intermediate black hole or a second stellar disk (Löckmann et al. 2009; Yu et al. 2007; Haas et al. 2011; Mapelli et al. 2013). Whether such objects exist/had existed in such configurations as to influence the evolution of the stellar disk is still actively studied.

Madigan et al. (2009) considered the collective eccentric disk instability effect. Such effect could lead to rapid change in the distribution of eccentricities in the disk, but it requires initially highly eccentric disk (see also Gualandris et al. 2012). Such a process may give rise to a significant population of highly eccentric stars in the disk; which are not seen in most recent studies (Yelda et al. 2014).

It is important to note that by their nature, most of the collective and secular effects mentioned above affect both low mass and high mass stars in a similar manner, leading to similar eccentricity distribution. Discerning the kinematic properties of low mass vs. high mass stars is therefore highly important in order to understand the roles of such processes compared with stellar two-body relaxation processes that lead to mass stratification, as shown here in details. In particular, non-dependence of the stellar kinematics on the stellar masses would strongly suggest collective effects dominate the stellar disk evolution.

6.6 Comparison with observations of the Galactic center

The observed eccentricity of O-stars in the stellar disk in the GC, $\langle e \rangle = 0.27 \pm 0.07$ (Yelda et al. 2014), is higher than that obtained in the realistic models considered here. This suggest either initial conditions with significantly higher eccentricities for the disk stars, or that other processes besides two-body relaxation play an important role in the disk evolution.

Detailed studies of the eccentricity/inclination distribution of disk stars as a function of mass is not currently available, (but see Madigan et al. 2014 for important global statistical trends). Moreover, lower mass B-stars in these regions may have a different origin than the disk, and may have been captured following a binary disruption (Perets et al. 2007); such stars would have high eccentricities (Perets & Gualandris 2010) and may mask the real distribution of the disk stars eccentricities. Nevertheless, a focused study on stars most likely related to the disk, and their eccentricity-mass relation is highly desirable to asses the existence of possible mass stratification in the stellar disk.

Finally, two body relaxation processes suggest a factor of two ratio between the eccentricities and inclination of stars in the disk, while different relation might be expected from other processes (e.g. secular Kozai-like evolution induced by an inclined massive structure). A good handle on the eccentricity vs. inclination from

observation could give additional clues on the dynamical processes involved.

7 SUMMARY

In this study we analyzed the evolution of a stellar disk around a massive black hole due to two-body relaxation processes and binary heating. We explored realistic mass functions for the disk stars, and included the effects of two-body relaxation by the nuclear cluster stellar population in which the disk is embedded. We also considered the effects of stellar evolution and studied the long term evolution of such disks. The disk evolution is dominated by dynamical friction from the massive stars in the disk, while binary heating plays only a negligible role in the disk evolution. The nuclear cluster plays a minor role in the disk evolution as long as a large population of massive stars exist, as in the case of a young disk with a top-heavy mass function; it can play a more significant, though still modest role in heating a disk with a Salpeter mass function. Due to stellar evolution the effective mass-function of the disk becomes progressively centered around lower mass stars and stellar remnants which replace the previously existing massive stars. Correspondingly, disk heating by the nuclear cluster plays a progressively more dominant role in the disk evolution.

We find that significant mass stratification arises from mass-segregation processes in the disk. This could serve as a signature for two-body relaxation dominating the disk evolution. In contrast, collective and secular effects are typically insensitive to the masses of individual stars in the disk, and would not produce mass stratification.

The observed RMS eccentricity of the O-stars in the stellar disk in the Galactic center (~ 0.27) is larger than obtained in any of our models with realistic conditions, suggesting either an initially hot and/or eccentric disk or that other secular/collective effects play an important role in the disk evolution.

REFERENCES

- Aharon D., Perets H. B., 2015, *ApJ*, 799, 185
 Alexander R. D., Begelman M. C., Armitage P. J., 2007, *ApJ*, 654, 907
 Alexander T., Pfuhl O., 2014, *ApJ*, 780, 148
 Amaro-Seoane P., Chen X., 2014, *ApJ Lett.*, 781, L18
 Antonini F., Perets H. B., 2012, *ApJ*, 757, 27
 Bahcall J. N., Wolf R. A., 1976, *ApJ*, 209, 214
 Bahcall J. N., Wolf R. A., 1977, *ApJ*, 216, 883
 Bartko H., Martins F., Fritz T. K., Genzel R., Levin Y., Perets H. B., Paumard T., Nayakshin S., Gerhard O., Alexander T., Dodds-Eden K., Eisenhauer F., Gillessen S., Mascetti L., Ott T., Perrin G., Pfuhl O., Reid M. J., Rouan D., Sternberg A., Trippe S., 2009, *ApJ*, 697, 1741
 Bartko H., Martins F., Trippe S., Fritz T. K., Genzel R., Ott T., Eisenhauer F., Gillessen S., Paumard T., Alexander T., Dodds-Eden K., Gerhard O., Levin Y., Mascetti L., Nayakshin S., Perets H. B., Perrin G., Pfuhl O., Reid M. J., Rouan D., Zilka M., Sternberg A., 2010, *ApJ*, 708, 834
 Binney J., Tremaine S., 2008, *Galactic Dynamics: Second Edition*. Princeton University Press
 Chabrier G., 2001, *ApJ*, 554, 1274
 Cuadra J., Armitage P. J., Alexander R. D., 2008, *MNRAS*, 388, L64
 Dale J. E., Davies M. B., Church R. P., Freitag M., 2009, *MNRAS*, 393, 1016
 Do T., Ghez A. M., Morris M. R., Lu J. R., Matthews K., Yelda S., Larkin J., 2009, *ApJ*, 703, 1323
 Freitag M., Amaro-Seoane P., Kalogera V., 2006, *ApJ*, 649, 91
 Genzel R., Eisenhauer F., Gillessen S., 2010, *Reviews of Modern Physics*, 82, 3121
 Goldreich P., Lithwick Y., Sari R., 2004, *ARA&A*, 42, 549
 Gualandris A., Mapelli M., Perets H. B., 2012, *MNRAS*, 427, 1793
 Haas J., Šubr L., Vokrouhlický D., 2011, *MNRAS*, 416, 1023
 Heggie D. C., 1975, *MNRAS*, 173, 729
 Hills J. G., 1975, *AJ*, 80, 809
 Hills J. G., 1992, *AJ*, 103, 1955
 Hobbs A., Nayakshin S., 2009, *MNRAS*, 394, 191
 Hopman C., 2009, *ApJ*, 700, 1933
 Hopman C., Alexander T., 2006a, *ApJ*, 645, 1152
 Hopman C., Alexander T., 2006b, *ApJ Lett.*, 645, L133
 Kocsis B., Tremaine S., 2011, *MNRAS*, 412, 187
 Kroupa P., 2002, *Science*, 295, 82
 Levin Y., Beloborodov A. M., 2003, *ApJ Lett.*, 590, L33
 Löckmann U., Baumgardt H., Kroupa P., 2009, *MNRAS*, 398, 429
 Lu J. R., Ghez A. M., Hornstein S. D., Morris M. R., Becklin E. E., Matthews K., 2009, *ApJ*, 690, 1463
 Madigan A.-M., Levin Y., Hopman C., 2009, *ApJ Lett.*, 697, L44
 Madigan A.-M., Pfuhl O., Levin Y., Gillessen S., Genzel R., Perets H. B., 2014, *ApJ*, 784, 23
 Mapelli M., Gualandris A., Hayfield T., 2013, *MNRAS*, 436, 3809
 Martins F., Trippe S., Paumard T., Ott T., Genzel R., Rauw G., Eisenhauer F., Gillessen S., Maness H., Abuter R., 2006, *ApJ Lett.*, 649, L103
 Merritt D., 2010, *ApJ*, 718, 739
 Ott T., Eckart A., Genzel R., 1999, *ApJ*, 523, 248
 Ozernoi L. M., Dokuchaev V. I., 1982, *A&A*, 111, 1
 Paumard T., Genzel R., Martins F., Nayakshin S., Beloborodov A. M., Levin Y., Trippe S., Eisenhauer F., Ott T., Gillessen S., Abuter R., Cuadra J., Alexander T., Sternberg A., 2006, *ApJ*, 643, 1011
 Perets H. B., 2009a, *ApJ*, 690, 795
 Perets H. B., 2009b, *ApJ*, 698, 1330
 Perets H. B., Gualandris A., 2010, *ApJ*, 719, 220
 Perets H. B., Gualandris A., Merritt D., Alexander T., 2008, *Mem. Societa Astronomica Italiana*, 79, 1100
 Perets H. B., Hopman C., Alexander T., 2007, *ApJ*, 656, 709
 Perets H. B., Kupi G., Alexander T., 2008, in Vesperini E., Giersz M., Sills A., eds, *IAU Symposium Vol. 246 of IAU Symposium, Getting a Kick out of the Stellar Disk(s) in the Galactic Center*. pp 275–276
 Perets H. B., Šubr L., 2012, *ApJ*, 751, 133
 Prodan S., Antonini F., Perets H. B., 2015, *ApJ*, 799, 118
 Rafelski M., Ghez A. M., Hornstein S. D., Lu J. R., Morris M., 2007, *ApJ*, 659, 1241
 Rauch K. P., Tremaine S., 1996, *New A*, 1, 149
 Salpeter E. E., 1955, *ApJ*, 121, 161
 Sana H., de Mink S. E., de Koter A., Langer N., Evans C. J., Gieles M., Gosset E., Izzard R. G., Le Bouquin J.-B., Schneider F. R. N., 2012, *Science*, 337, 444
 Stewart G. R., Wetherill G. W., 1988, *Icarus*, 74, 542
 Yelda S., Ghez A. M., Lu J. R., Do T., Meyer L., Morris M. R., Matthews K., 2014, *ApJ*, 783, 131
 Yu Q., Lu Y., Lin D. N. C., 2007, *ApJ*, 666, 919